Eur. J. Biochem. *257*, 337−343 (1998)

Resolution of the heterogeneous fluorescence in multi-tryptophan proteins: ascorbate oxidase

Almerinda DI VENERE[1], Giampiero MEI[1], Gianfranco GILARDI[2], Nicola ROSATO[1], Fabio DE MATTEIS[3], Robert McKAY[4], Enrico GRATTON[5] and Alessandro FINAZZI AGRÒ[1]

[1] Department of Experimental Medicine and Biochemical Sciences, University of Rome 'Tor Vergata', Rome, Italy
[2] Department of Biochemistry, Imperial College of Science, Technology and Medicine London, UK
[3] Department of Physics, University of Rome 'Tor Vergata', Rome, Italy
[4] Department of Biochemistry and Biophysics, University of Hawaii, Honolulu, USA
[5] Laboratory for Fluorescence Dynamics, Department of Physics, University of Illinois at Urbana-Champaign, Illinois, USA

(Received 15 April/5 June 1998) − EJB 98 0514/3

Ascorbate oxidase is a copper-containing enzyme which catalyzes a redox reaction between vitamin C and molecular oxygen. The protein, which shows a complex tertiary structure, is an homodimer of monomers, each containing three domains and 14 tryptophan residues. Recently, we have demonstrated by spectroscopic and ultracentrifugation techniques the existence of a stable dimeric intermediate along the unfolding pathway of this enzyme [Mei, G., Di Venere, A., Buganza, M., Vecchini, P., Rosato, N. & Finazzi Agrò, A. (1997) *Biochemistry 36*, 10917−10922]. In this study, the steady-state and dynamic fluorescence features of ascorbate oxidase have been exploited in order to find a way of monitoring the individual subsystems of the protein. The fluorescence intensity and anisotropy upon excitation at 295 nm are extremely sensitive functions of the emission wavelength, indicating a great heterogeneity of the system. The emission decay collected through a cut-off filter can be analyzed in terms of two continuous distributions of lifetimes. Using a monochromator in emission or an optical multichannel analyzer, the two distributions may be attributed to distinct components of the fluorescence spectrum. Differential quenching by cesium chloride also confirmed that the several tryptophan residues present in the protein structure may be grouped into two main classes, each with a different environment. Once the complex fluorescence decay of ascorbate oxidase was analyzed and resolved, a comparison with the crystallographic data allowed a first, approximate attribution of the protein spectroscopic properties to some of the tryptophan residues. This might provide a powerful tool of investigation about the role of definite segments of the protein in its three-dimensional structure and catalytic activity. Furthermore, the methodology set up for ascorbate oxidase can be usefully extended to other multitryptophan proteins.

Keywords: lifetime distribution; time-resolved emission spectroscopy; fluorescence quenching; red-edge excitation.

Fluorescence techniques have been widely used to characterize both the conformation and the dynamic behaviour of large biological structures such as membranes and proteins. For proteins, the presence of intrinsic probes (tyrosine and tryptophan residues) with lifetime values in the range of nanoseconds, allows a detailed study of processes which occur at the microscopic level. In particular, the development of time-resolved methods, the improvement of light sources and data-analysis software offer the possibility of collecting accurate data about protein conformational fluctuations and enzyme-substrate interactions. Several authors [1−4] have described dynamic fluorescence decays of proteins in terms of continuous distributions of lifetimes. This model of data analysis is related to the heterogeneity of the tryptophan or tyrosine microenvironments [5, 6]. The mobility of the aromatic residues accounts, at least in part, for this heterogeneity since the fluorophores may experience several different microscopic states during their lifetime. Tryptophan in a rigid environment has a fluorescence decay which can be fitted by a sum of discrete components [7, 8]. In contrast, accurate anisotropy measurements on protein dynamics have provided evidence for segmental motions occurring in a time range of nanoseconds or less. Interconversion among the substates of a hierarchically organized protein structure [9] may be a further reason for heterogeneous fluorescence decay. Another important factor which may contribute to spread a single lifetime into a continuous distribution of lifetimes is the so called 'red-edge' effect due to solvent relaxation around the excited fluorophore [10, 11]. As this process occurs during the excited state, red-edge fluorescence spectroscopy may be a suitable technique to monitor local dynamics, especially in the case of single fluorophore-containing proteins. However, when many tryptophan residues are present, a discrimination between solvent relaxation and intrinsic heterogeneity of the system can be hardly made.

Correspondence to A. Finazzi Agrò, Department of Experimental Medicine and Biochemical Sciences, University of Rome 'Tor Vergata', Via di Tor Vergata 135, I-00133 Rome, Italy
Fax: +39 6 20427292.
E-mail: MEI@utovrm.it

Abbreviations. AAO, ascorbate oxidase; TRES, time-resolved emission spectroscopy; OMA, optical multichannel analyzer; $AcTrpNH_2$, *N*-acetyl-tryptophanamide.

Enzyme. Ascorbate oxidase (EC 1.10.3.3).

Note. This paper is dedicated to the memory of W. E. Blumberg and G. Weber who introduced us to the shining beauty of fluorescence.

Site-directed mutagenesis has recently allowed the spectrum of a multi-tryptophan-containing protein to be dissected into its components [12−16]. However, when the size and the complexity of the system is such that mutants cannot be properly expressed and assembled, other indirect methods might be proposed.

We have studied several spectroscopic features of ascorbate oxidase (AAO), a multi-copper enzyme which catalyses one-electron oxidation of vitamin C with the simultaneous four-electron reduction of molecular oxygen to water [17]. Crystallographic data have shown that ascorbate oxidase is a dimeric globule of identical subunits each containing three distinct domains. AAO is spectroscopically very complex because it has 23 tyrosine residues and 14 tryptophan residues per monomer. However, the fluorescence intensity and anisotropy have been extensively used to study the unfolding of AAO by guanidinium hydrochloride and urea [18]. It was demonstrated that the unfolding pathway is complex, including the formation of a stable, dimeric, intermediate species. Nevertheless, a better knowledge of the AAO spectroscopic properties is required to study the stability of AAO in solution, the interaction between its subunits (long-range interactions) and the subdomains folding (short-range interactions).

In this paper, we attempted to dissect the contribution of different fluorophores to the emission spectrum of AAO using steady-state and dynamic fluorescence, and time-resolved emission spectroscopy (TRES) [19]. Red-edge excitation, polarization spectra (as a function of temperature and viscosity) and the effect of fluorescence quenching agents such as acrylamide and CsCl allowed the detection of two distinct classes of fluorescent tryptophan residues.

MATERIALS AND METHODS

Materials. Ascorbate oxidase from green zucchini was purchased from Boehringer Mannheim Biochemicals and its purity was checked by gel electrophoresis. The protein was dissolved in 80 mM potassium-phosphate, pH 6.0. Glycerol (for fluorescence microscopy) was purchased from Merck KGaA. In all experiments, the samples were kept at the desired temperature using an external circulating bath (HAAKE, model CH-F3).

Steady-state fluorescence measurements. Steady-state fluorescence measurements were carried out with a single-photon-counting spectrofluorometer (ISS, model K2). The bandwidth of excitation and emission monochromators varied in the range 2−4 nm. For all the fluorescence experiments, the optical absorbance of the samples, at 280 nm or at 295 nm, was in the range 0.10−0.15. The spectra were corrected using an instrument correction curve obtained with standard fluorescent compounds such as *N*-acetyl tryptophanamide ($AcTrpNH_2$) and *N*-acetyl tyrosinamide.

All fluorescence-quenching measurements were corrected for the inner-filter effect. To simulate the absorption of quencher molecules at the excitation and the emission wavelengths, two cuvettes (5 mm optical length), containing a solution of quenchers in buffer, were placed along the excitation and emission pathways. The fluorescence of $AcTrpNH_2$ was thus measured varying the concentration of quencher and two correction curves (one for each quencher) were obtained. In order to evaluate the amount (f_a) of fluorophore accessible to the quencher molecules as well as the quenching constant of CsCl, a non-linear fit of the data was performed using the following equation:

$$\frac{F_0}{\Delta F} = \frac{1}{f_a K[Q]} + \frac{1}{f_a} \quad (1)$$

where F_0 is the fluorescence in absence of quenchers, $\Delta F = F_0 - F$ is the difference between the signals in absence and in presence of CsCl, K is the dynamic or static quenching constant and [Q] is the quencher concentration. Eqn (1), which describes the quenching of two population of fluorophores, one of which being inaccessible for the quencher, was derived as described elsewhere [20].

Dynamic fluorescence measurements. Dynamic fluorescence measurements were performed using the phase-shift and demodulation technique at the Laboratorio di Spettroscopia ai Picosecondi, LASP (University of Rome, 'Tor Vergata', Italy). The samples were excited at ≈293 nm using as excitation source the harmonic content of a mode-locked Nd-Yag laser, as previously described [21].

All the results were analyzed by minimizing the reduced χ^2 with routines based on the Marquardt algorithm using the Globals Unlimited Software [22].

Time-resolved emission spectra. The data were acquired using a time-resolved diode array detector (model KADStar by ISS Inc.) at the Laboratory for Fluorescence Dynamics, LFD, (University of Illinois at Urbana-Champaign, USA). The fluorescence light was collected by a fiber bundle 2-m long and 5-mm in diameter; the bundle was made of 200 μm diameter, ultraviolet-grade quartz fibers. The bundle transported the fluorescence light to a polychromator (320 mm focal length, *F*/5.4 aperture with 58 mm×58 mm grating) which acted as a dispersing element of the fluorescence spectrum. An image intensifier and 2048 linear array detector were mounted at the exit slit of the polychromator. The fluorescence light impinging onto the photocathode of the image intensifier was amplitude-modulated using a radio frequency signal whose phase was locked with the radiofrequency signal modulating the excitation light beam. The cross-correlation frequency (the difference between the frequency of the two radiofrequency signals) was 8 Hz. In this way, the low-frequency component of the signal (at 8 Hz) passed through the phosphor of the image intensifier and was collected by the array detector. An acquisition card inserted into the computer acquires the data using the ISS Oma Optical Multichannel Analyzer Software, for the on-line calculation of the phase shifts and demodulation of the fluorescence at each element of the array detector. The highest modulation frequency of this instrument is about 180 MHz; typical lifetime resolution of this detector is about 200 ps.

Analysis of the protein structure. The crystallographic data have been analyzed using both visual inspection and more accurate quantitative routines such as Insight II in which the external surface of the whole protein is explored and the exposed area of the aromatic residues is calculated. This procedure has been repeated twice, once for the dimeric and once for the monomeric structures.

RESULTS AND DISCUSSION

Steady-state measurements. The steady-state emission spectra of AAO upon excitation at two different wavelengths, namely 280 nm and 293 nm, were normalized to 100 (Fig. 1). The superposition of the two spectra in the blue-edge indicates that the tyrosine-residues contribution to the overall emission is almost negligible, probably because a very efficient energy transfer to tryptophan residues is occurring. Instead, the small difference in the red-edge and the breadth of the spectrum indicate an emission heterogeneity. Indeed, the emission peak is centered at ≈321 nm but a shoulder may be observed at ≈337 nm.

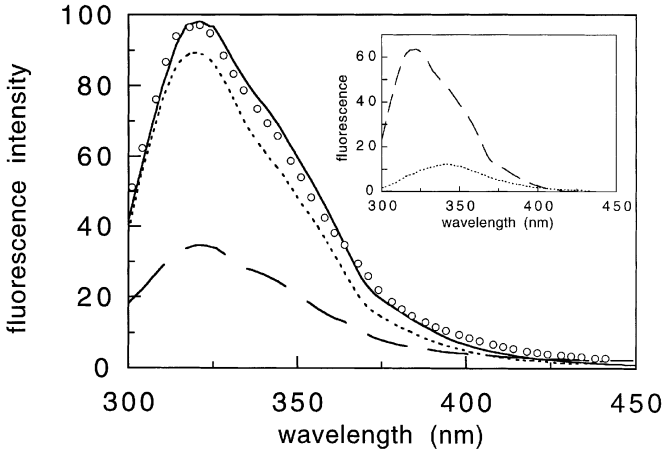

Fig. 1. Fluorescence spectrum of AAO. Steady-state emission spectra of AAO excited at 280 nm (open circles) and 293 nm (solid line) in buffer (normalized to 100) or in the presence of 1.3 M CsCl (dotted line) and 0.5 M acrylamide (dashed line). Inset: difference spectra between AAO excited at 293 nm and AAO in presence of 1.3 M CsCl (dotted lines) or 0.5 M acrylamide (dashed lines).

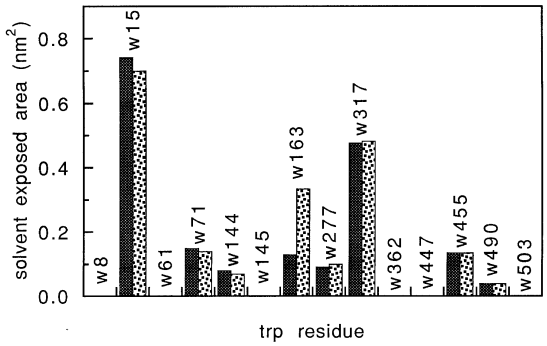

Fig. 2. Solvent exposed areas of the 14 tryptophan residues in a single AAO subunit. Filled and dashed bars represent the areas calculated on the dimeric and monomeric crystallographic structures, respectively.

Since these two emission wavelengths are typical of buried and partially buried tryptophan residues in proteins [23], it may be argued that most emitting tryptophan residues belong to these categories. X-ray crystallographic data [24, 25] show that most of the 14 tryptophan residues in each subunit are located in hydrophobic regions (Fig. 2). In particular, six tryptophan residues/monomer are completely shielded from the solvent (W8, W61, W145, W362, W447 and W503); six tryptophan residues (W71, W144, W163, W277, W455 and W490) are also rather buried since their exposed area is 0.05−0.15 nm^2; finally, only two of them (W15 and W317) are exposed to the solvent. These data allow a preliminary classification of the fluorophores in different groups, characterized by emission properties corresponding to different microenvironments. A spectroscopical heterogeneity of the system was also observed by measuring the steady-state anisotropy, $\langle r \rangle$, as a function of the emission wavelength upon excitation at 295 nm and 25 °C. This parameter is practically constant when only fluorophores with identical properties are present. Instead, an almost linear decrease of the $\langle r \rangle$ value is observed for AAO (Fig. 3A). This behaviour can be attributed to at least two different situations, namely an energy transfer from buried to exposed tryptophan residues or a greater mobility (possibly associated with longer lifetime values) of the red-emitting

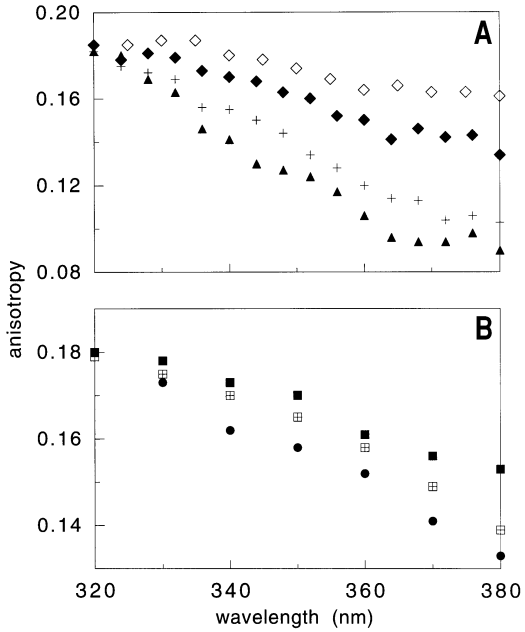

Fig. 3. Fluorescence anisotropy dependence on temperature and viscosity. (A) Steady-state emission anisotropy upon excitation at 295 nm at 25 (filled diamonds), 45 (crosses) or 55 °C (filled triangles). Open diamonds represent the anisotropy measured in presence of 1.3 M CsCl at 25 °C. (B) Steady-state anisotropy of AAO at 30 °C (circles) and in the presence of 10 % and 20 % glycerol (open and filled squares, respectively). The experimental error (not reported for the sake of clarity) was $\Delta r \approx \pm 0.002$.

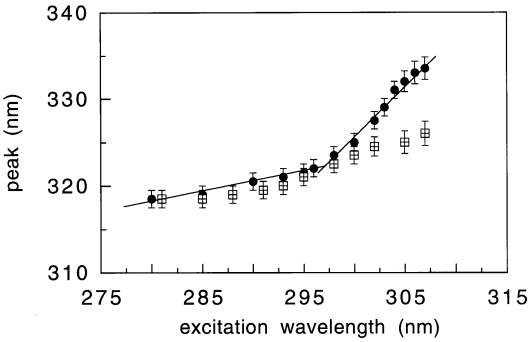

Fig. 4. Red-edge fluorescence emission of AAO. Maximum fluorescence emission versus excitation wavelength for AAO (circles) and for AAO in presence of 1.3 M CsCl (squares). Solid lines represent the best linear fits of circles.

fluorophores. In order to test which hypothesis might hold in this case, the anisotropy was measured at higher temperatures, namely 45 °C and 55 °C. Here, the decrease in the anisotropy was steeper at longer wavelengths, leveling off beyond 365 nm (Fig. 3A). In the presence of CsCl, which quenches the solvated tryptophan residues, a relevant increase in the anisotropy value was observed at the red edge of the fluorescence spectrum (Fig. 3A). This result suggests that the decrease in $\langle r \rangle$ values at longer emission wavelengths might be related to peculiar properties of the red-emitting tryptophan residues.

The effect of viscosity on the $\langle r \rangle$ value was studied at 30 °C by adding glycerol to the solution. The anisotropy observed at the red edge of the fluorescence spectrum (Fig. 3B) increases at increasing glycerol concentrations. Even though energy transfer among tryptophan residues cannot be ruled out, these findings

Table 1. Quenching parameters. λ_{max} is the position of the maximum fluorescence emission; $\Delta\lambda$ the width at half maximum of the fluorescence spectrum. (f_a^s) and (f_a^d) are the amounts of quenched fluorophores evaluated on the basis of the Stern-Volmer plots reported in Fig. 5. The values were obtained by steady-state and dynamic fluorescence measurements, respectively. Finally, K_S and K_D represent the Stern-Volmer quenching constants obtained from steady-state and dynamic fluorescence measurements.

Sample	λ_{max}	$\Delta\lambda$	f_a^s	K_S	f_a^d	K_D
	nm			M^{-1}		M^{-1}
AAO	321 ± 1	55 ± 1	–	–	–	–
AAO + acrylamide	321 ± 1	55 ± 1	1.00	3.19 ± 0.06	1.00	3.12 ± 0.09
AAO + CsCl	319 ± 1	52 ± 1	0.18 ± 0.01	1.7 ± 0.1	0.19 ± 0.01	1.7 ± 0.4

indicate that the heterogeneity of the fluorescence spectrum mainly depends on the greater mobility of the solvated fluorophores. Thus, assuming that the heterogeneity of the fluorescence signal was essentially due to distinct contributions of two different classes of fluorophores, we expected to find a strong dependence of the steady-state emission spectrum on the excitation energy. A biphasic behaviour of the emission peak is observed and two linear functions are required to fit the data (Fig. 4). While, by exciting up to 295 nm, the peak slowly moves to longer emission wavelengths, above ≈297 nm this dependence becomes steeper and, within 10 nm (297−307 nm) the spectrum shifts to the red by about 11 nm. This effect might be correlated to a significantly different exposure of the two classes of tryptophan residues to the solvent. In fact, when the experiment is carried out in the presence of CsCl, two slopes are still visible but the difference is much less pronounced (Fig. 4). Further quenching experiments have also been performed using acrylamide in order to explore the solvent accessibility of the different tryptophan residues. The spectra obtained at the highest concentration of quencher used (Fig. 1; λ_{ex} = 293 nm) and the related spectroscopic parameters (Table 1) show that although acrylamide has the greatest quenching effect, it does not affect the width or the peak position of the spectrum. A different result was obtained with CsCl which mainly quenches the long-wavelength-emitting tryptophan residues. This quencher is able to shift the spectrum maximum by about 2 nm to higher energy and to narrow the width of the spectrum at half maximum intensity (Table 1). The difference spectra in the absence and in the presence of quenchers (Fig. 1) indicate how the CsCl effect is restricted to the exposed tryptophan residues, characterized by an emission at ≈343 nm and associated to the abrupt variation of slope (Fig. 4).

The Stern-Volmer data obtained with acrylamide (Fig. 5A) can be fitted to a straight line while with CsCl (Fig. 5B) nonlinearity is shown. This behaviour of the Stern-Volmer plot has been generally interpreted by the presence of two classes of fluorophores, one of which is inaccessible to the quencher [26]. The data (Fig. 5B) have been fitted according to this hypothesis (see Materials and Methods) and the parameters of the best fit are reported in Table 1. The amount of quenched fluorophores extrapolated at infinite denaturant concentration is 100% for acrylamide and about 17−18% for CsCl. Considering that 28 tryptophan residues/AAO dimer are present, the accessibility measured at 1.3 M CsCl (≈13.2%) corresponds approximately to two tryptophan residues/monomer if, as a first approximation, the same fluorescence intensity is assumed for all fluorophores. Indeed, this result seems in fair agreement with the crystallographic data analysis (Fig. 2), which pointed to W15 and W317 as the best candidates for the red-emitting class of fluorophores.

Fluorescence-decay measurements. The heterogeneity observed in the steady-state measurements is associated to a com-

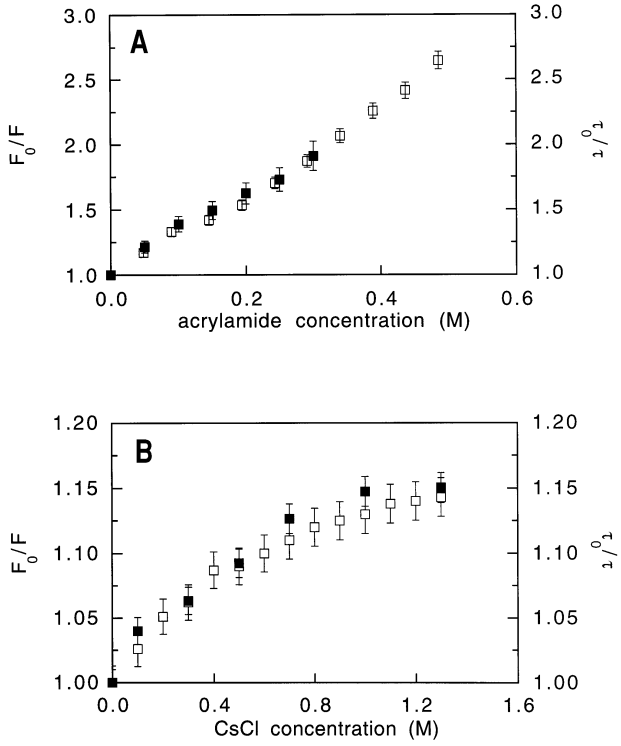

Fig. 5. Acrylamide and CsCl quenching effects on the AAO emission properties. Steady-state (open squares) and dynamic (filled squares) quenching of AAO by acrylamide (A) and CsCl (B) upon excitation at 293 nm.

plex fluorescence decay. The decay data of AAO fluorescence studied by phase and modulation have been fitted using different models, namely 1, 2 and 3 exponentials or 1 and 2 lorentzian distributions of lifetimes (Table 2). In agreement with the best χ^2 value and the best weighted residuals (data not shown), the bimodal lorentzian distribution appeared to be more appropriate to describe the decay (Fig. 6A). The soundness of this approach, which might also be justified by the large number of tryptophan residues, can be checked by the successful interpretation of the data. Indeed, a complex decay may have, in principle, different origins. Distributed fluorescence decays have been already reported even in the case of single fluorophore-containing proteins [27, 6, 28]. It was proposed that the width of the distribution may reflect the number of the protein conformational substates experienced by the fluorophore during the excited state [1, 29]. For AAO, the presence of several tryptophan residues is evidently a source of complexity. The distributions of lifetimes reported (Fig. 6A) may be used to evaluate the relative fractions

Table 2. Fluorescence decay parameters for AAO. C is the fluorescence lifetime (i.e., center of lorentzian distribution if w_1 or w_2 are reported). $\Delta C_1 \approx 30$ ps; $\Delta C_{2,3} \approx 50$ ps; w is the width of lorentzian distribution ($\Delta W_{1,2} \approx 40$ ps) and F the fractional intensity associated to each lifetime component ($\Delta F_{1,2,3} \approx 0.01$). χ^2 is the reduced chi-squared of phase and modulation data fit.

Fitting function	C_1	W_1	F_1	C_2	W_2	F_2	C_3	F_3	χ^2
	ns			ns			ns		
1 exponential	1.26	–	1.00	–	–	–	–	–	668.2
1 lorentzian	1.05	1.88	1.00	–	–	–	–	–	16.0
2 exponentials	0.51	–	0.42	2.64	–	0.58	–	–	5.5
2 lorentzians	0.55	0.93	0.53	2.48	0.45	0.47	–	–	1.0
3 exponentials	0.32	–	0.27	1.70	–	0.55	4.70	0.18	1.2

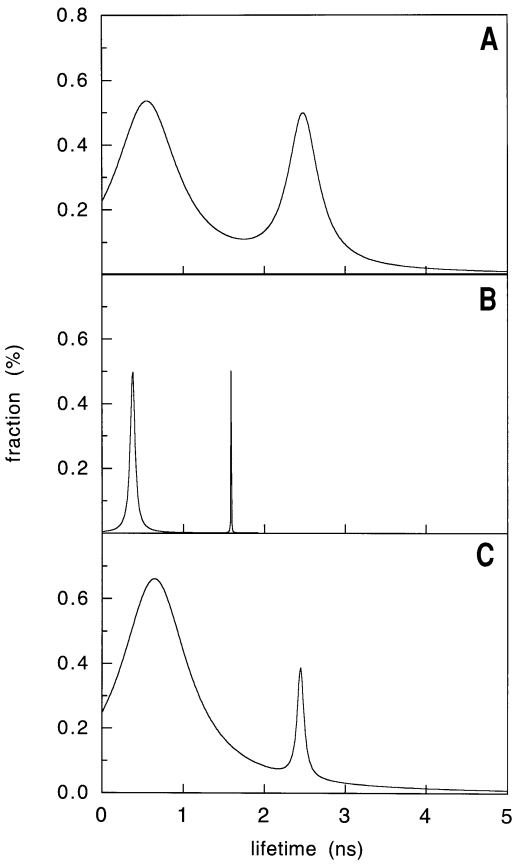

Fig. 6. AAO fluorescence lifetime distributions. Emission was collected using a cut-off filter at 305 nm (A) and in presence of 0.3 M acrylamide (B) or 1.3 M CsCl (C).

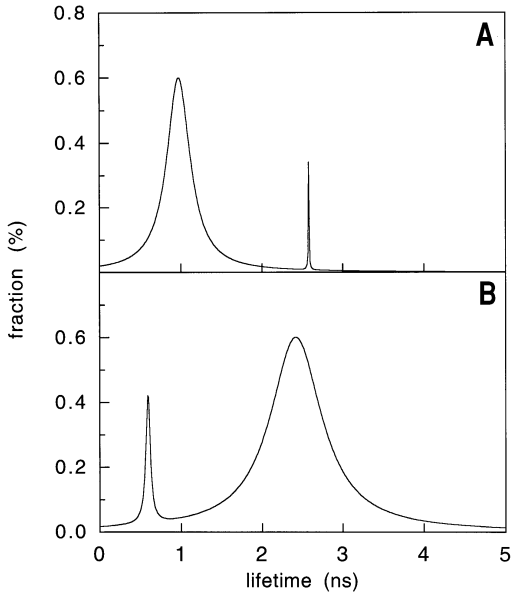

Fig. 7. Profiles of fluorescence lifetime distributions using an emission monochromator (bandwidth = 4 nm) set at 320 nm (A) or at 350 nm (B).

of the two tryptophan populations, i.e. the pre-exponential factors of the fluorescence decay. This calculation yields 0.84 for the first population and 0.16 for the longer lifetimes species, which parallel fairly well, within the experimental error, the ratio of 12:2 obtained from the CsCl quenching experiment and from the crystallographic analysis. In order to ascertain whether each distribution might be ascribed to a particular set of fluorophores, the fluorescence decay was also measured in the presence of quenchers. Both the widths and the centers of the two distributions are dramatically affected by the presence of 0.3 M acrylamide (Fig. 6B). A Stern-Volmer plot of the τ_0/τ ratio, i.e. the average lifetime in the absence and in the presence of acrylamide, is reported in Fig. 5A together with the steady-state measurements. Again, a linear dependence may be observed confirming that this neutral quencher has accessibility to almost all the fluorescent tryptophan residues of AAO. The fluorescence decay of AAO is also influenced by CsCl. However, in this case, only the lifetimes components around 2–3 ns are affected (Fig. 6C) indicating that the tryptophan residues accessible to the CsCl molecules are associated for the longer component of the decay. The corresponding dynamic Stern-Volmer plot is reported in Fig. 5B. The overlap of the two data sets indicates that only a dynamic process is occuring [26]. The non-linearity is, in fact, similar to that observed by the steady-state measurements from which the same amount of quenched tryptophan residues (≈18%) has been evaluated (Table 1).

The internal domains of proteins are generally highly hydrophobic. The different effects of charged and neutral quenchers is considered to be a consequence of their different penetrations into the protein matrix. Our experiments with CsCl point out that most tryptophan residues in AAO are inaccessible to positive (Cs^+) ions which, instead, quenched the exposed residues although with a different efficiency due to the presence of different number of charged amino acid residues around the exposed tryptophan residues [24, 25]. A different value of the bimolecular quenching constant for Trp15 and Trp317, due to this different net charge, can also explain the small decrease of the center and the consistent narrowing of the width of the lifetime distribution. Thus, the dynamic quenching data are consis-

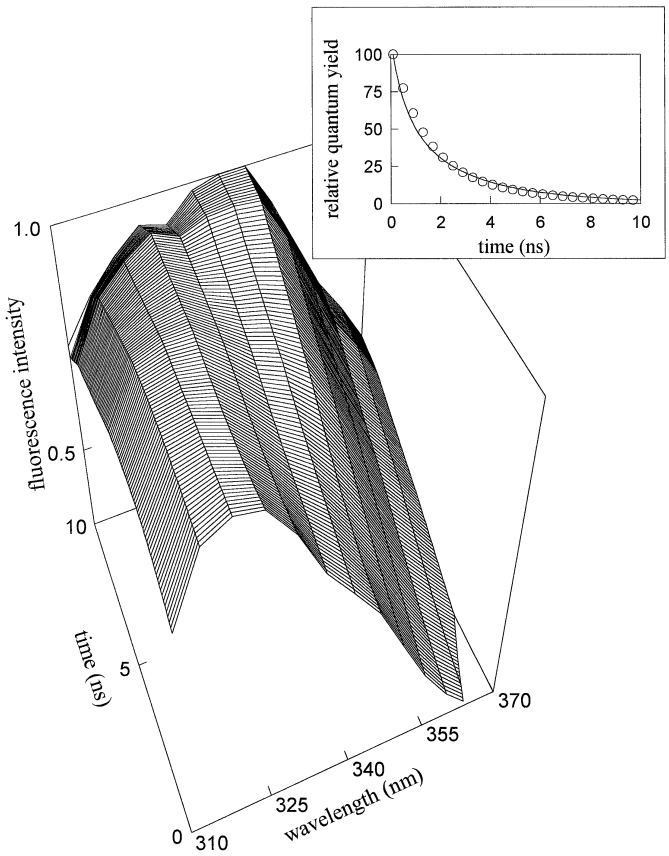

Fig. 8. TRES obtained using an optical multichannel analyzer. For better clarity, the spectra have been normalized to 1. Inset: comparison between the relative quantum yield of the TRES spectra (open circles) and the calculated number of emitted photons as a function of time (solid line).

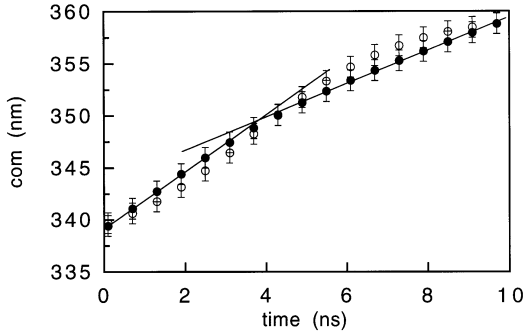

Fig. 9. Center of mass of the time resolved emission spectra of AAO (filled circle) and center of mass calculated as a linear combination of two different emitting species as described in the text (open circles).

tent with the presence of two classes of fluorophores, and also give information on the polarity of the respective environments. The dependence of the fluorescence lifetimes on the emission wavelength has been studied by collecting the phase and modulation data through an emission monochromator and performing the measurements at several wavelengths. The results of the best fit obtained in the blue (320 nm) and red (350 nm) regions of the AAO emission spectrum are reported in Fig. 7 A and B. The wavelength selection obtained by the monochromator allows each distribution to be assigned to a particular region of the spectrum. The red edge of the fluorescence spectrum showed a broader distribution around ≈2.5 ns (Fig. 7 B), while the shorter component is much narrower and shifted from 0.6 ns to 1.0 ns (Fig. 7 A). The latter effect is probably due to the monochromator which cuts off the emission at wavelengths shorter than 315 nm. This possible artifact was overcome using an optical multichannel analyzer (OMA) as described in Materials and Methods. In this way, the dependence of the fluorescence lifetimes on the emission wavelength has been analyzed in more detail and the time-resolved emission spectra of AAO have been evaluated. The profile of the spectrum as a function of time (Fig. 8) confirms that the blue part of the AAO spectrum is associated with short fluorescence lifetimes, while the slower decay corresponds to tryptophan residues emitting at longer wavelengths. These results are consistent with those reported by Kouyama et al. [30].

In order to check the correspondence between the distribution analysis and time-resolved emission spectroscopy (TRES), the average number of emitted photons as a function of time has been calculated from the lorentzian functions (Fig. 6 A). The two sets of data are superimposable (Fig. 8).

The spectrum at $t = 0$ ns evolves to that at the longest observed time in a biphasic way, (Fig. 9) where the center of mass of TRES has been reported. To check whether this time dependence of the spectrum may originate from two distinct populations of fluorophores, TRES has been simulated using a simple model where the emission spectrum of AAO was fitted with the linear combination of two species. The first one, which represents the blue-emitting tryptophan residues, was assumed to peak at 319 nm with a full width at half maximum of ≈52 nm, chosen on the basis of the CsCl-quenching experiment (Table 1 and Fig. 1, dotted curve). The other species is that represented by the difference spectrum (Fig. 1, dotted line). It has a peak at ≈343 nm, a full width at a half maximum of ≈56 nm and corresponds to the spectrum of the tryptophan residues quenched by CsCl. Two different radiative rate constants, corresponding to the centers of the lorentzian distributions (Table 2 and Fig. 6 A), have been associated with each spectrum, and the center of mass of the time-resolved emission spectra have been re-evaluated by the sum of two distinct decays and compared with those obtained for the TRES. The correspondence between the experimental and the calculated TRES is fairly good (Fig. 9) confirming the assumption that the overall emission of AAO is indeed the linear combination of the emissions of two different types of tryptophan residues.

CONCLUSIONS

This study shows that it is possible to separate the fluorescence contribution of different classes of fluorescent residues in very complex proteins such as AAO. In particular, the data of fluorescence decay, collected as a function of the emission wavelength (OMA), provide new support for the interpretation of dynamic fluorescence in terms of continuous distributions of lifetimes. Two classes of tryptophan residues have been identified in AAO from their steady-state and dynamic-fluorescence properties. The spectroscopic data nicely fit the three-dimensional structure of AAO obtained by X-ray crystallography, indicating that the protein in solution and in the crystalline lattice has the same interaction with the solvent. These results give structural information which might be useful for a dynamic characterization of the AAO dimeric intermediate state found in its unfolding pathway, which is underway in our laboratory. As a more general application, this methodology can be extended to other multi-tryptophan-containing proteins. In particular, whenever the crystallographic structure are unknown, a combination of the described methodology with site-directed mutagenesis

could be a straightforward strategy to analyze the intrinsic heterogeneity of the protein fluorescence spectrum.

We thank the staff of the LASP laboratory at the University of Rome, 'Tor Vergata', and the staff of the LFD at the University of Urbana Champaign. The authors also acknowledge Dr Beniamino Barbieri from I.S.S. company (USA) for technical assistance. This work has been partially sponsored by Science Programme EEC grant no. 90-0434 and NIH 6M.

REFERENCES

1. Alcala, R., Gratton, E. & Prendergast, F. (1987) Interpretation of fluorescence decays in proteins using continuous lifetime distributions, *Biophys. J. 51*, 925−936.
2. Gentin, M., Vincent, M., Brochon, J. C., Livesey, A. K., Cittanova, N. & Gallay, J. (1990) Time-resolved fluorescence of the single tryptophan residue in rat alpha-fetoprotein and rat serum albumin: analysis by the maximum-entropy method, *Biochemistry 29*, 10405−10412.
3. Vincent, M., Li De La Sierra, I. M., Berberan-Santos, M. N., Diaz, A., Diaz, M., Padron, G. & Gallay, J. (1992) Time-resolved fluorescence study of human recombinant interferon alpha2. Association state of protein, spatial proximity of the two tryptophan residues, *Eur. J. Biochem. 210*, 953−961.
4. Mei, G., Pugliese, L., Rosato, N., Toma, L., Bolognesi, M. & Finazzi Agrò, A. (1994) Biotin and biotin analogues specifically modify the fluorescence decay of avidin, *J. Mol. Biol. 242*, 559−565.
5. Lakowicz, J. R., Cherek, H., Gryczynski, I., Joshi, N. & Johnson, M. L. (1987) Analysis of fluorescence decay kinetics measured in the frequency domain using distributions of decay times, *Biophys. Chem. 28*, 35−50.
6. Ferreira, S. T., Stella, L. & Gratton, E. (1994) Conformational dynamics of bovine Cu, Zn Superoxide Dismutase revealed by time-resolved fluorescence spectroscopy of the single tyrosine residue, *Biophys. J. 66*, 1185−1196.
7. Gryczynski, I., Eftink, M. & Lakowicz, J. R. (1988) Conformation heterogeneity in proteins as an origin of heterogeneous fluorescence decays, illustrated by native and denaturated ribonuclease T_1, *Biochim. Biophys. Acta 954*, 244−252.
8. Gilardi, G., Mei, G., Rosato, N., Canters, G. W. & Finazzi Agrò, A. (1994) Unique environment of Trp48 in *Pseudomomas aeruginosa* azurin as probed by site-directed mutagenesis and dynamic fluorescence spectroscopy, *Biochemistry 33*, 1425−1432.
9. Frauenfelder, H., Sligar, S. G. & Wolynes, P. G. (1991) The energy landscapes and motions of proteins, *Science 254*, 1598−1603.
10. Lakowicz, J. R. & Keating-Nakamoto, S. (1984) Red edge excitation of fluorescence and dynamic properties of proteins and membranes, *Biochemistry 23*, 3013−3021.
11. Demchenko, A. P. (1986) *Ultraviolet spectroscopy of proteins*, Springer-Verlag, Berlin Heidelberg.
12. Martineau, P., Szmelcman, S., Spurlino, J. C., Quiocho, F. A. & Hofnung, M. (1990) Genetic approach to the role of tryptophan residues in the activities and fluorescence of a bacterial periplasmic maltose-binding protein, *J. Mol. Biol. 214*, 337−352.
13. Royer, C. A. (1992) Investigation of the structural determinants of the intrinsic fluorescence emission of the trp repressor using single tryptophan mutants, *Biophys. J. 63*, 741−750.
14. Wasylewski, Z., Koloczek, H., Wasniowska, A. & Slizowska, K. (1992) Red-edge excitation fluorescence measurements of several two-tryptophan-containing proteins, *Eur. J. Biochem. 206*, 235−242.
15. Willaert, K., Loewenthal, R., Sancho, J., Froeyen, M., Fersht, A. & Engelborghs, Y. (1992) Determination of the excited-state lifetimes of tryptophan residues in barnase, via multifrequency phase fluorometry of tryptophan mutants, *Biochemistry 31*, 711−716.
16. Hasselbacher, A., Rusinova, E., Waxman, E., Rusinova, R., Kohanski, R. A., Lam, W., Guha, A., Du, J., Lin, T. C., Polikarpov, I., Boys, C. W. G., Nemerson, Y., Konigsberg, W. H. & Ross, J. B. A. (1995) Environments of the four tryptophans in the extracellular domain of human tissue factor: comparison of results from absorption and fluorescence difference spectra of tryptophan replacement mutants with the crystal structure of the wild-type protein. C, *Biophys J. 69*, 20−29.
17. Malkin, R. & Malström, B. G. (1970) The state and function of copper in biological systems, *Adv. Enzymol. 33*, 177−243.
18. Mei, G., Di Venere, A., Buganza, M., Vecchini, P., Rosato, N. & Finazzi Agrò, A. (1997) Role of quaternary structure in the stability of dimeric proteins: the case of ascorbate oxidase, *Biochemistry 36*, 10917−10922.
19. Beechem, J. M., Gratton, E., Ameloot, M., Knutson, J. R. & Brand, L. (1991) The global analysis of fluorescence intensity and anisotropy decay data: second-generation theory and programs, in *Topics in fluorescence spectroscopy* (Lakowicz, J. R., ed.) vol. 2, pp. 241−305, Plenum Press, NY-London.
20. Lehrer, S. S. (1971) Solute perturbation of protein fluorescence. The quenching of the tryptophan fluorescence of model compounds and of lysozyme by iodide ion, *Biochemistry 10*, 3254−3263.
21. Gratton, E. & Limkeman, M. (1983) A continuosly variable frequency cross-correlation phase fluorometer with picosecond resolution, *Biophys. J. 44*, 315−324.
22. Beechem, J. M. & Gratton, E. (1988) Fluorescence spectroscopy data analysis environment: a second generation global analysis program, *Proc. SPIE-INT. Soc. Opt. Eng. 909*, 70−81.
23. Burstein, E. A., Vedenkina, N. S. & Ivkova, M. N. (1973) Fluorescence and the location of tryptophan residues in protein molecules, *Photochem. Photobiol. 18*, 263−279.
24. Messerschmidt, A., Rossi, A., Ladenstein, R., Huber, R., Bolognesi, M., Gatti, G., Marchesini, A., Petruzzelli, R. & Finazzi Agrò, A. (1989) X-ray crystal structure of the blue oxidase ascorbate oxidase from zucchini, *J. Mol. Biol. 206*, 513−529.
25. Messerschmidt, A., Ladenstein, R., Huber, R., Bolognesi, M., Avigliano, L., Petruzzelli, R., Rossi, A. & Finazzi Agrò, A. (1992) Refined crystal structure of ascorbate oxidase at 1.9 Å resolution, *J. Mol. Biol. 224*, 179−205.
26. Lakowicz, J. R. (1983) *Principles of fluorescence spectroscopy*, Plenum Press, NY-London.
27. Mei, G., Rosato, N., Silva, N. Jr, Rusch, R., Gratton, E., Savini, I. & Finazzi Agrò, A. (1992) Denaturation of human Cu/Zn superoxide dismutase by guanidine hydrochloride: a dynamic fluorescence study, *Biochemistry 31*, 7224−7230.
28. Bouhss, A., Vincent, M., Munier, H., Gilles, A. M., Takahashi, M., Bârzu, O., Danchin, A. & Gallay, J. (1996) Conformational transitions within the calmodulin-binding site of *Bordetella pertussis* adenylate cyclase studied by time-resolved fluorescence of Trp242 and circular dichroism, *Eur. J. Biochem. 237*, 619−628.
29. Ware, R. W. (1992) Recovery of fluorescence lifetime distributions in heterogeneous systems, in *Photochemistry in organized and constrained media* (Ramamurthy, V., ed.) pp. 563−602, VCA Publisher, New York.
30. Kouyama, T., Kinosita, K. Jr & Ikegami, A. (1989) Correlation between internal motion and emission kinetics of tryptophan residues in proteins, *Eur. J. Biochem. 182*, 517−521.